

Nanometer targeting of microtubules to focal adhesions

Olga Krylyshkina,¹ Kurt I. Anderson,² Irina Kaverina,¹ Irene Upmann,³ Dietmar J. Manstein,³ J. Victor Small,¹ and Derek K. Toomre⁴

¹Institute of Molecular Biology, Salzburg A5020, Austria

²Max Planck Institute of Molecular Cell Biology and Genetics, 01307 Dresden, Germany

³Biophysics Department, Max Planck Institute for Medical Research, D-69120 Heidelberg, Germany

⁴Department of Cell Biology, Ludwig Institute for Cancer Research, Yale University School of Medicine, New Haven, CT 06520

Although cell movement is driven by actin, polarization and directional locomotion require an intact microtubule cytoskeleton that influences polarization by modulating substrate adhesion via specific targeting interactions with adhesion complexes. The fidelity of adhesion site targeting is precise; using total internal reflection fluorescence microscopy (TIRFM), we now show microtubule ends (visualized by incorporation of GFP tubulin) are within 50 nm of the substrate when polymerizing toward the cell periphery, but not when shrinking from it. Multiple microtubules sometimes followed similar tracks, suggesting

guidance along a common cytoskeletal element. Use of TIRFM with GFP- or DsRed-zyxin in combination with either GFP-tubulin or GFP-CLIP-170 further revealed that the polymerizing microtubule plus ends that tracked close to the dorsal surface consistently targeted substrate adhesion complexes. This supports a central role for the microtubule tip complex in the guidance of microtubules into adhesion foci, and provides evidence for an intimate cross-talk between microtubule tips and substrate adhesions in the range of molecular dimensions.

Introduction

Cell polarity is lost or impaired when microtubules are depolymerized, indicative of a cross-talk between microtubules and the actin cytoskeleton in cell polarization (Vasiliev, 1985). It is now generally thought that microtubules exert their polarizing role by transducing signals in a spatial way to the actin cytoskeleton, but ideas of the nature of the signals and the means of their transduction are diverse (Geiger and Bershadsky, 2001; Wittmann and Waterman-Storer, 2001; Gundersen, 2002; Kaverina et al., 2002a; Small et al., 2002). One possible route of signal transduction was suggested by conventional fluorescence microscopy, which showed that microtubules

grow over and into adhesion complexes, where the actin cytoskeleton couples to the substrate (Kaverina et al., 1998). Moreover, it was found that such adhesion site-targeting events by microtubules could be correlated with adhesion complex turnover or adhesion release (Kaverina et al., 1999). Therefore, the suggestion was made that microtubules confer polarity on the actin cytoskeleton by modulating, in a spatially regulated way, the pattern of substrate adhesions (Kaverina et al., 1999). To directly evaluate the spatial fidelity of targeting, we have exploited the technique of total internal reflection fluorescence microscopy (TIRFM).*

Results and discussion

In TIRFM (Axelrod, 1989; Steyer and Almers, 2001; Toomre and Manstein, 2001), also called evanescent wave microscopy, the excitation light typically penetrates <150 nm above the reflecting surface and is ideal for studying cellular processes that take place close to the growth substrate, such as cell adhesion (Truskey et al., 1992) and exocytosis (Steyer

The online version of this article includes supplemental material.

Address correspondence to Derek K. Toomre, Dept. of Cell Biology, Ludwig Institute for Cancer Research, Yale University School of Medicine, 333 Cedar Street, PO Box 208002, New Haven, CT 06520. Tel.: (203) 785-4319. Fax: (203) 785-3559. E-mail: derek.toomre@yale.edu; or J.V. Small, Austrian Academy of Sciences, Institute of Molecular Biology, Dept. of Cell Biology, Billrothstrasse 11, Salzburg A5020, Austria. Tel.: 43-662-63961-11. Fax: 43-662-63961-40. E-mail: jvsmall@imb.oeaw.ac.at

I. Upmann and D.J. Manstein's present address is Institute for Biophysical Chemistry, OE 4350, and Central Unit for Biochemical and Biophysical Systems, OE 8830, Medizinische Hochschule Hannover, D-30623 Hannover, Germany.

Key words: cytoskeleton; CLIP-170; TIRFM; zyxin; cross-talk

*Abbreviation used in this paper: TIRFM, total internal reflection fluorescence microscopy.

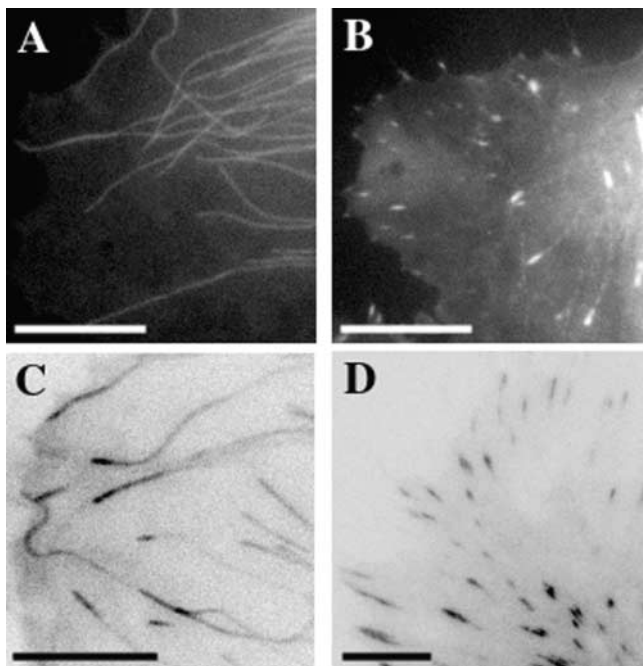


Figure 1. TIRFM reveals microtubule tips and focal adhesions within 150 nm of the dorsal cell surface. CAR fibroblasts were transfected with either GFP-tubulin (A and C) or GFP-zyxin (B and D). Live-cell images were taken either with standard wide field epi-illumination (A and B) or TIRFM (C and D). For clarity, TIRFM images are shown in reverse contrast. Bar, 10 μm . For C, see also Video 1 and Video 2.

and Almers, 2001; Toomre and Manstein, 2001). In Fig. 1, images of live cells are shown transfected with either GFP-tubulin or -zyxin (an adhesion site component) obtained using conventional fluorescence microscopy (Fig. 1, A and B) and TIRFM (Fig. 1, C and D); for clarity, TIRFM images are presented in negative contrast. In TIRFM, microtubules showed a graded intensity of fluorescence along their length, with the brightest fluorescence at the growing tips situated toward the cell edge, indicative of a “dipping down” of microtubules toward the substrate, into the zone of exponentially increasing illumination of the evanescent wave (<150 nm). Zyxin is known to reside at substrate adhesion sites, and occasionally displays a periodic labeling along larger stress fiber bundles (Fig. 1 B); in TIRFM, only the ventral adhesion sites were observed (Fig. 1 D), suggesting that ventral stress fibers lie predominately above the zone excited by the evanescent wave.

To highlight the approach of the microtubules toward the cell surface, a false colored image, mapped to a rainbow look-up table, is shown in Fig. 2 A. Note that the plus end tips show a relatively bright and constant intensity over μm -sized segments, suggesting that they are “riding” near the dorsal cell cortex. An advantage of TIRFM is that as the fluorescence intensity decreases as $\sim 1/e$ away from the surface (Axelrod, 1989), small changes in z -position give a large change in signal, and the relative or even absolute position of the object can be determined along the z -axis. Representative images in Fig. 2 B show that close contact typically extends along the XY plane from ~ 5 – 20 μm , and the micro-

tubules observed here generally approached the surface at a relatively shallow angle ($<5^\circ$). Notably, and as shown in Fig. 2 B, the plus end microtubule tips approached to within 50 nm of the substrate.

Live-cell TIRFM imaging of microtubule dynamics revealed two striking phenomena. The first was a consistent difference in the distance of the tips of microtubules from the substrate during phases of growth and shrinkage (Fig. 3, A and B; Video 1 and Video 2, available at available at

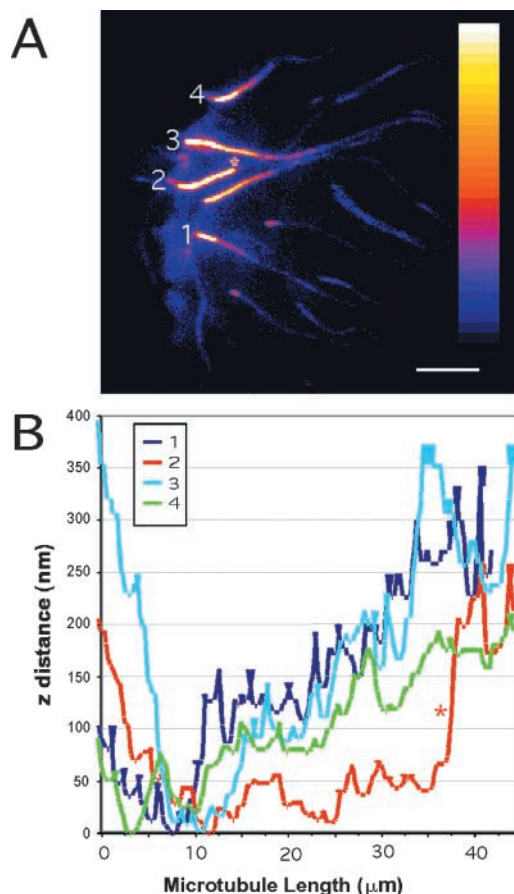


Figure 2. Approach of microtubule plus end tips to the cell surface.

(A) CAR fibroblasts transfected with GFP-tubulin and imaged by TIRFM (as in Fig. 1 C) were false colored to highlight the change in fluorescence intensity along the microtubule. No pixels were saturated. Bar, 10 μm . (B) The intensity of four microtubules (labeled 1–4 in A) was measured along the microtubules starting near the extreme plus end (near number). Based on an exponential drop-off in fluorescence intensity as an inverse exponential away from the surface ($1/e$ = penetration depth) the relative distance of the microtubules to the cell surface was calculated and plotted as a line trace (0 = plus end). Traces were also taken in regions not containing microtubules to correct for the local background (not depicted). Note that close contact of the microtubule plus end with the cell surface over several micrometers; gradually, the intensity drops as the microtubules enter deeper into the cell (right side). In this temporal “snapshot,” there are both polymerizing and depolymerizing microtubules, and the extreme plus end often “lifts off” before the microtubule depolymerizes (see Video 1 and Video 2). Most microtubules approach the surface at a shallow angle of $<5^\circ$, although occasionally the angle of attack was observed as steep as $\sim 10^\circ$, e.g., in the region marked with a red asterisk.

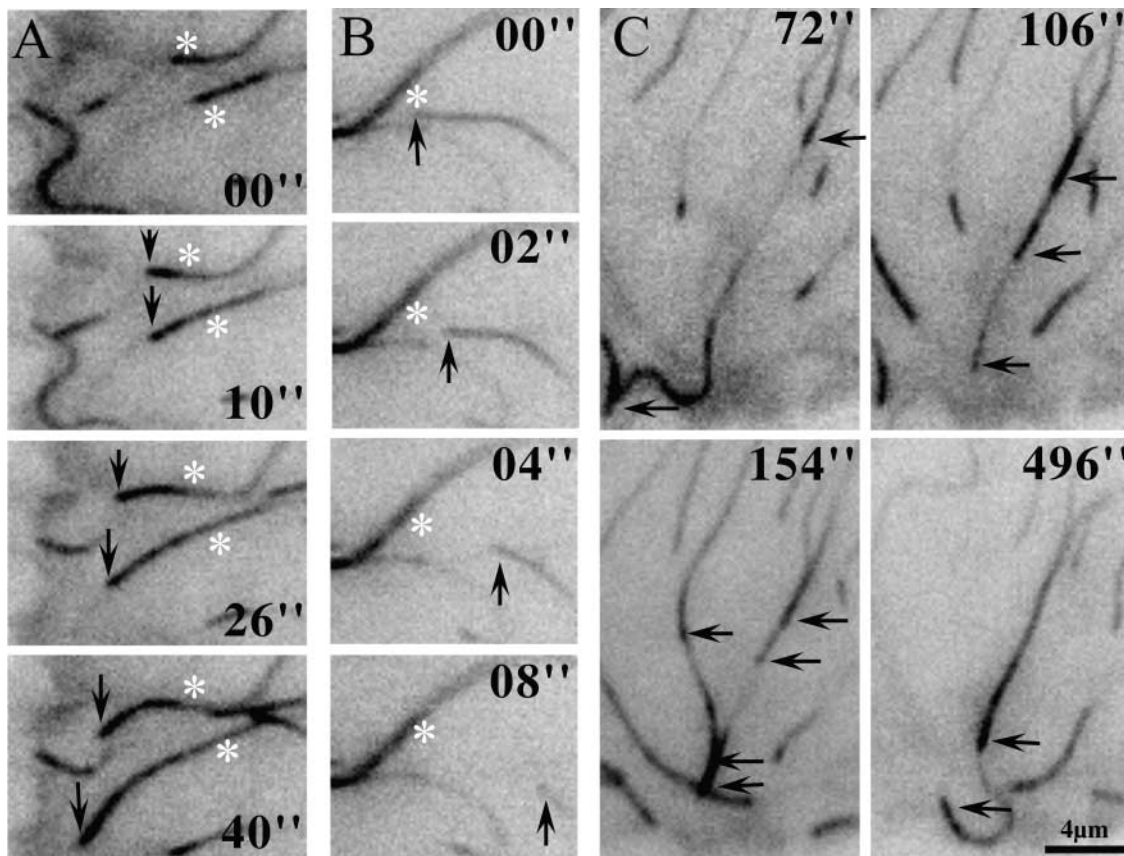


Figure 3. Observation of microtubule plus ends by TIRFM indicates that microtubules lift away from the substrate during shrinkage, and shows microtubule tracking along common paths. (A–C) Higher magnification views of individual time-lapse frames from Fig. 1 C. (A) Growing microtubule plus ends as observed by TIRFM. The asterisk marks the position of the microtubule ends in the first frame, and the arrows follow the microtubule growth in subsequent frames. Note that the microtubules “dip down” and form a close contact with the cell cortex during microtubule elongation, as seen by the difference in fluorescent intensity along the microtubule. (B) A representative example of a shrinking microtubule. Note the loss of close contact of the microtubule with the cell matrix as it shrinks. (C) Microtubules were observed to follow common tracks appearing to piggy-back along each other, sometimes with three or more following a common track. The arrows mark microtubules that follow common tracks (see also Video 1 and Video 2).

<http://www.jcb.org/cgi/content/full/jcb.200301102/DC1>. This was indicated by intensity measurements that showed that shrinking microtubule ends within the evanescent zone were $\sim 45 \pm 12\%$ as intense as growing ends (data from 21 microtubules, both in growing and shrinking phases). Second, microtubules often tracked along the same paths during polymerization toward a common point at the cell edge (Fig. 3 C; Video 1 and Video 2). Indeed, up to four microtubules were observed to follow the same track. This phenomenon is consistent with the existence of structural elements that can guide microtubule polymerization in peripheral regions. Alternatively, secondary and tertiary microtubules may “piggy-back” along a primary microtubule. Either way, this suggests that a primary targeting event can create a cue for subsequent targeting events along a common path. Similar microtubule dynamics and tracking was also observed in mammalian cells (PtK2) by TIRFM (unpublished data).

The spatial interaction between microtubules and substrate adhesions, first described using conventional microscopy (Kaverina et al., 1998), was vividly confirmed by dual-color TIRFM. In cells cotransfected with GFP-tubulin and DsRed-zyxin, video analysis revealed that the dipping of mi-

croto- tubules toward the substrate was invariably associated with the targeting of adhesion sites (Fig. 4 A and Video 3). Examples of different types of targeting events are highlighted in Fig. 4 (B and C) and the accompanying videos (Video 4 and Video 5). Video sequences were acquired by recording images every second, for a total time of ~ 1 –4 min. Within such short periods, multiple targeting events could be recorded (Fig. 4 A and Video 3). By the use of inverted colors, the high intensity of microtubule plus end-terminal regions during approach to focal adhesions was made more readily apparent (Fig. 4 A and Video 3).

However, do these growing microtubule ends represent “sliding” events or the “new polymerization” of microtubule plus ends? The dynamics of microtubule polymerization can be independently assessed by using specific fluorescently tagged proteins that accumulate at the growing tips of microtubules (Schroer, 2001; Schuyler and Pellman, 2001). Several of these proteins, including CLIP-170, the first described among microtubule tip proteins (Rickard and Kreis, 1990), dissociate from the plus ends of microtubules when polymerization ceases (Perez et al., 1999). In Fig. 5 (A and B), video frames are shown of cells cotransfected with DsRed-zyxin and GFP-CLIP-170; for illustra-

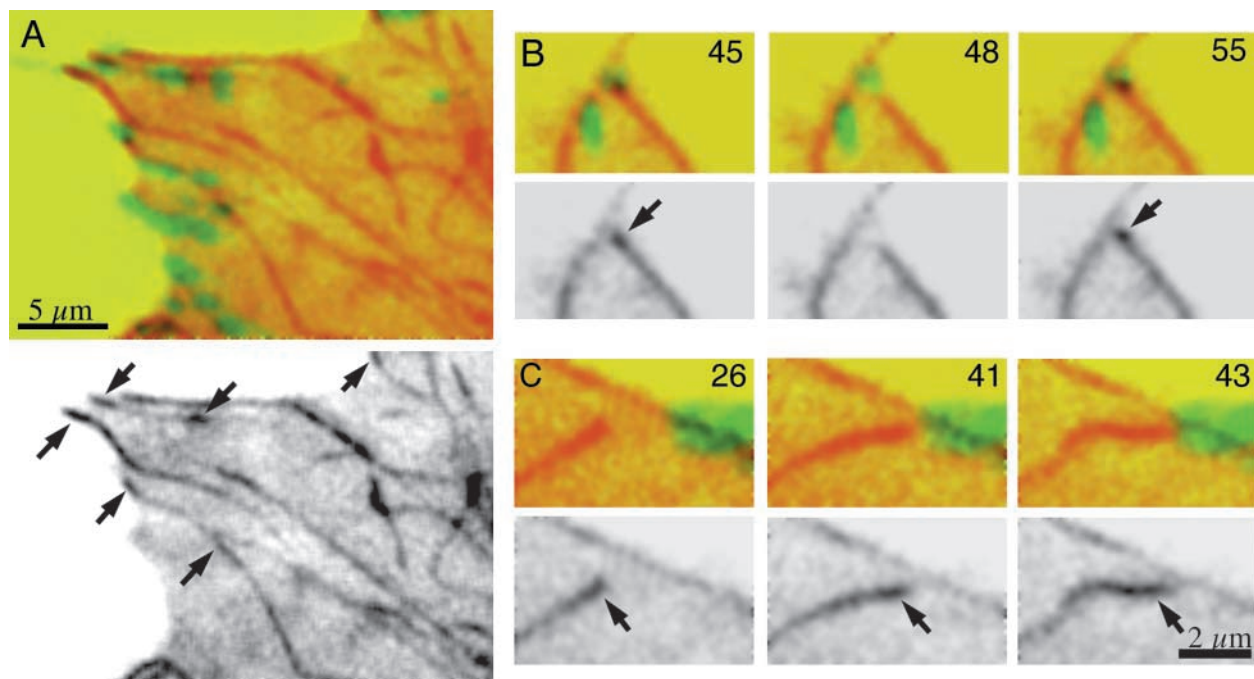


Figure 4. Nanometer targeting of microtubules to focal adhesions revealed by TIRFM. Video frames in TIRFM of CAR fibroblasts double transfected with DsRed-zyxin and GFP-tubulin. Pseudocolors have been used to facilitate visualization of adhesions (zyxin, green) and microtubules (tubulin, red). Single-channel GFP-tubulin images are shown in black and white. (A) An overview of the edge of the cell showing microtubule-adhesion targeting (top) and, on the bottom, the approach of a number of microtubules tips to the substrate in positions colocalizing with adhesion sites (arrows). (B and C) Other examples of microtubules dipping down to adhesion complexes; time shown in seconds (see also Videos 3–5).

tive purposes, tracks of GFP-CLIP-170 labeled microtubule tips (Mimori-Kiyosue et al., 2000) are shown in Fig. 5 C for individual microtubules (Fig. 5 B, pencil arrows). In the dual-color confocal time-lapse series (Fig. 5 A) and accompanying video (Video 6), CLIP-170 remained associated with the tips of microtubules en route to peripheral adhesions, marked by zyxin. This clearly shows that targeting involves the polymerization (and not sliding) of microtubules into adhesion complexes. In dual-color TIRFM (Fig. 5, B and C; Video 7), labeling with GFP-CLIP-170 showed again, and perhaps even more vividly than with GFP-tubulin (Fig. 5 D and Video 8), that the routing of microtubule polymerization into adhesion foci involved the tracking of growing microtubule tips inside the region excited by the evanescent wave that is within 150 nm of the dorsal surface.

In earlier works, we have noted that microtubules can specifically target single adhesion sites within a closely spaced group of adhesions (Kaverina et al., 1998, 1999). The high precision of this targeting, now shown by TIRFM, is presumably necessary to restrict the spatial cross-talk between microtubules and adhesions to allow modulation of the turnover of single adhesion foci. The fact that successive microtubules can follow the same tracks into adhesion sites is consistent with guidance of microtubule polymerization along another cytoskeletal element that terminates in adhesion complexes. Speculations about how this may occur have been aired previously (Kaverina et al., 1998; Small and Kaverina, 2003) and, in the context of the present findings, are presented schematically in Fig. 5 E.

The most likely candidate for the guidance track is actin because microtubule targeting also occurs in cells lacking intermediate filaments (Kaverina et al., 1998). One possible means of guidance is already suggested by recent findings in budding yeast (Yin et al., 2000) where the directed polymerization of microtubules into the bud involves a myosin V homologue, resident in the microtubule tip complex. This is an attractive possibility because we have shown that microtubule polymerization is stimulated by an increase in stress in the actin cytoskeleton (Kaverina et al., 2002b), suggesting that microtubules may track along actin filaments that are under tension (Fig. 5 E). A myosin motor at the microtubule tip could readily serve as a mechanosensor in this process by recognizing actin filaments whose conformation or composition are modified under stress. Alternatively, or simultaneously, another coupling component (Fig. 5 E, boxed region) may be involved that binds both microtubules and actin filaments. A number of proteins have been described that bind both actin and microtubules (Gavin, 1997), but it remains to be shown whether such a cross-linker resides at microtubule tips, where guidance must be initiated. Further studies are aimed at testing these alternative guidance scenarios.

The dipping down of polymerizing microtubules into adhesion sites, revealed by evanescent wave microscopy, can be explained in terms of docking of microtubules onto an actin track that leads to a substrate adhesion site (Fig. 5 E). In the same context, the rapid lifting of microtubules away from the substrate on shrinkage may reflect the release of the microtubule tip from the same track. Lifting is

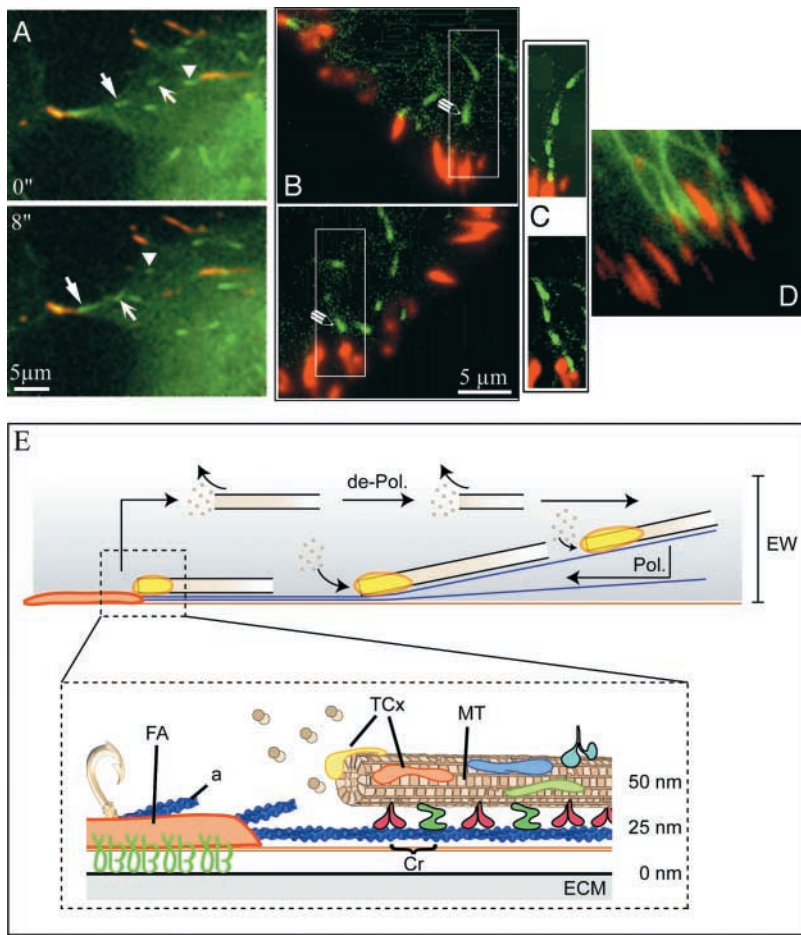


Figure 5. Polymerization of microtubule tips into adhesion sites. (A) Confocal video frames of CAR fibroblast transfected with DsRed-zyxin and GFP-CLIP-170. Different arrowhead pairs mark the tips of three microtubules en route to an adhesion complex. Times are in seconds. (B) Video images of a cell transfected as in A, but imaged instead by TIRFM, showing the close proximity of polymerizing microtubule tips to the dorsal cell surface (note that the high contrast TIRFM has much less background and microtubule plus ends (green) are seen in the evanescent field). (C) A merge of five time points (over 20 s) from the boxes in B shows the microtubules polymerizing toward the adhesion markers (red). (D) Dual-color TIRFM imaging of a cell transfected with GFP-tubulin and DsRed-zyxin. Cell region is similar to the one shown in B (see also Videos 6–8). (E) Working model of the guidance of microtubules into focal adhesions. Top part shows side view of guidance scenario highlighting the striking differences in Z-axis position of microtubule plus ends during polymerization (Pol.) and depolymerization (de-Pol.). Microtubule polymerization is directed down to an adhesion site and into the evanescent wave (EW) by the docking of the microtubule tip complex onto an actin track. Depolymerization away from the adhesion site is associated with the loss of the tip complex and the lifting of the microtubule away from the track and the substrate. Depolymerizing microtubules can go through rescue and reenter the polymerizing cycle to retarget the adhesion site through dynamic instability. Bottom part shows boxed region scaled to approximate molecular dimensions. The focal adhesion (FA) and axis of the microtubule (~24 nm in diameter) are drawn 15 and 50 nm away from the substrate, respectively.

The numerous known tip complex proteins (TCx) likely decorate the microtubule surface much more extensively than depicted. Coupling between microtubules and actin (a) is effected by a coupler complex (Cr) that is part of the microtubule tip complex, as proposed elsewhere (Small and Kaverina, 2003). The coupler could be an unconventional myosin or a microtubule-actin cross-linker (see text). Microtubules may be captured (hook) at the adhesion site. ECM, extracellular matrix.

commensurate with microtubule depolymerization, which is accompanied by the loss of tip proteins, consistent with a requirement of the microtubule tip complex in the guidance process (Fig. 5 E, boxed region). The significance of the present finding that microtubules interact with adhesion sites in a nanometer range (within ~50 nm) is best appreciated by considering the relative dimensions involved (Fig. 5 E, boxed region). Taking focal adhesions as themselves separated ~15 nm from the substrate, the diameter of microtubules as 24 nm, and a layer of proteins associated with microtubule plus ends (Schroer, 2001), the microtubule tip must approach adhesion sites close enough to allow an intimate cross-talk of molecular interactions. This intimacy may also form the basis of the capture of microtubule plus ends at the cell cortex, possibly involving the dynein-dynactin complex (Gundersen, 2002). Various molecules have been implicated in the cross-talk between microtubules and the actin cytoskeleton (Goode et al., 2000; Wittmann and Waterman-Storer, 2001; Kaverina et al., 2002a; Krendel et al., 2002; Small and Kaverina, 2003), but their relative roles remain to be defined. Further insights into this phenomenon will be facilitated by the exploitation of the TIRFM method in conjunction with

probes that reveal or modify the dynamics of the candidate molecules and complexes involved.

Materials and methods

Cells

Goldfish fin fibroblasts (line CAR, No. CCL71; American Type Culture Collection) were maintained in basal Eagle medium with HBSS, nonessential amino acids, and 15% FBS at 25°C.

Constructs

For expression of GFP-fused proteins, mouse β -tubulin in a pEGFP-C2 vector and human zyxin in a pEGFP-N1 vector were used. EGFP-zyxin (Rottner et al., 2001) and EGFP-tubulin were provided by Jurgen Wehland and coworkers (Gesellschaft für Biotechnologische Forschung, Braunschweig, Germany). DsRed-zyxin was a gift from Anna Huttenlocher (University of Wisconsin-Madison, Madison, WI), and GFP-CLIP-170 was donated by Anna Akhmanova (Erasmus University Rotterdam, Rotterdam, Netherlands).

Transfections

Subconfluent monolayer cultures of CAR cells plated on 30-mm Petri dishes were used for transfection. The transfection mixture was prepared as follows: 2 μ g DNA (1 μ g per construct) and 12 μ l SuperFect lipofection agent (QIAGEN) were mixed in 300 μ l serum-free medium. After incubation at RT for 30 min, an additional 1.2 ml of medium containing 5% serum was added. Cells were incubated in this mixture for 5 h and then replaced with normal medium. After 24 h, the cells were replated onto either 20-mm #1 glass coverslips or sapphire coverslips (Toomre et al., 2000;

1-mm thickness \times 32-mm diameter; Olympus) for TIRFM imaging with an objective-type and prism-type setup, respectively. Cells were used within 1–4 d of plating.

Microscopy

TIRFM imaging was performed using both prism- and objective-type TIRFM setups; both yielded similar results. The prism-type setup was used as described previously (Toomre et al., 2000), except imaging was performed at $\sim 25^\circ\text{C}$ as is optimal for imaging of fish fibroblasts. In brief, an upright microscope was used (Axiovert; Carl Zeiss MicroImaging, Inc.) fitted with a 60×1.25 NA water immersion lens (Carl Zeiss MicroImaging, Inc.). The 488-nm line of a krypton-argon laser was focused on the hemicylinder at an incident angle of 65° , giving a penetration depth $(1/e)$ of ~ 45 nm. Data were typically collected at 0.5–1 Hz.

A schematic of the objective-type TIRFM system is shown in Fig. S1. A difference with other objective-type setups is that two small prisms mounted below the objective lens were used to efficiently couple the laser beam into and out of the lens, and eliminated the need for dichroic filter. In brief, the 488-nm line from a 4-W argon laser (Spectra-Physics) was used for excitation. The laser was coupled via an acousto-optical modulator (ELS) into a single-mode 488-nm fiber (Point Source). At the outlet of the fiber, the beam was collimated with two achromatic doublet lenses ($f = 25.4$ mm and 300 mm; Newport) mounted on an optical rail and expanded to a diameter of 1.5 cm. A third achromatic doublet lens ($f = 500$ mm; Newport) focused the beam into the back focal plane of a $100\times$ objective lens (NA 1.40, Planachromat; Olympus) by reflecting off a 5-mm prism (OptoSigma). The beam exited the lens at an incident angle of $\sim 65 \pm 1^\circ$, giving a calculated penetration depth of 165 nm. The emitted light was filtered with an emission filter (HQ 545/45; Chroma), and was detected with a CCD camera (9.9×9.9 - μm pixels; SensiCam, PCO). Data were typically acquired at 0.5–1 Hz and were controlled with T.I.L.L. Photonics hardware and software.

Multi-channel TIRF

In brief, the system for multi-channel TIRFM consisted of a microscope (model IX2; Olympus) fitted with an IX2-RFAEVA condenser. A $100\times$ objective with NA of 1.65 was used in conjunction with high refractive index immersion oil (diodomethane; Sigma-Aldrich) and special high NA coverslips ($n = 1.788$; optical components from Olympus). The filter cube contained a 488/10 laser clean-up filter in the excitation position, a FT 510 dichroic filter, and an LP 520 emission filter. The excitation source was a multi-line laser (Innova 70C; Coherent) with an AOTF (acousto-optic modulator) for line selection and fast shuttering, coupled to the microscope using a kineFLEX fiber optic system (Point Source).

Laser excitation was performed at 488 nm, and the emission signals were separated using an optical splitter (MultiSpec; Optical Insights) with 595 dichroic, 515–565 BP, and 590 LP emission filters; the red and green images were simultaneously imaged side by side on a CCD camera (MicroMAX 1024B; Princeton Instruments). Images were acquired, and the raw stacks were split into single channels using MetaMorph[®] software (Universal Imaging Corporation).

Image processing and analysis

Post-acquisition processing was performed with TILLvisION software (T.I.L.L. Photonics), Microsoft Excel, Adobe Illustrator[®], ImageJ, and Adobe Photoshop[®]. Analyses of microtubule tips were performed using TILLvisION software to trace fluorescent intensities along the microtubule. The intensity values were exported to Microsoft Excel spreadsheets for correction of background fluorescence, conversion to relative z-position values, and graphing. TIRFM calculations were performed as described elsewhere (Axelrod, 1989; Toomre et al., 2000; Steyer and Almers, 2001).

Online supplemental material

Fig. S1 shows a schematic of TIRFM objective-type setup. Video 1 shows dynamics of microtubule plus end tips as visualized by TIRFM. This movie accompanies Fig. 1 C and Fig. 3, and shows an overview of GFP-tagged microtubules in CAR cells as imaged by TIRFM. The image is shown in reverse contrast. Note that as microtubule tips enter the evanescent wave the (plus end) tips appear darker. The real sample acquisition time is shown in seconds (time between frames = 2 s). Video 2 is the same as Video 1, except that is played back faster to highlight the observation that several microtubules travel along the same path. (time between frames = 2 s). Video 3 shows TIRFM visualization of microtubules targeting to adhesion sites. This movie accompanies Fig. 4 A and shows an overview of a CAR fibroblast double transfected with DsRed-zyxin and GFP-tubulin and imaged by

TIRFM. The single-color images have been thresholded, segmented, and color mapped to different intensities (using ImageJ software) to better distinguish microtubules from the adhesions and show their interaction. The top shows inverted RGB image (zyxin, green; tubulin, red) and the bottom shows only the GFP channel (microtubules) in inverted black and white. Real sample acquisition time is shown in seconds (time between frames = 2 s). Video 4 and Video 5 show individual microtubule targeting to adhesion sites. Individual examples of targeting interactions in TIRFM in CAR fibroblast double transfected with DsRed-zyxin and GFP-tubulin are shown and displayed like Video 3. Video 4 and Video 5 correspond respectively with images shown in Fig. 4, B and C. Note that the sequence highlights the dipping down of the microtubule plus ends toward focal adhesions. The real sample acquisition time is shown in seconds (time between frames = 1 s). Video 6 shows confocal images of microtubules polymerizing toward focal adhesions. This movie accompanies Fig. 5 A and shows CAR fibroblasts double transfected with DsRed-zyxin and GFP-CLIP-170 and acquired with a confocal laser scanning microscope (Radiance; Bio-Rad Laboratories). The GFP-CLIP-170 (green) is only seen on the growing microtubule plus ends, which can be seen to target focal adhesions (red). The real sample acquisition time is shown in seconds (time between frames = 2 s). Video 7 shows that dual-color TIRFM reveals microtubule plus end polymerizing toward and targeting focal adhesions. This movie accompanies Fig. 5 B and shows a CAR fibroblast double transfected with DsRed-zyxin and GFP-CLIP-170 and imaged by TIRFM. The high fluorescent intensity signal of CLIP-170-labeled tips indicates their close contact with the cell cortex, en route to adhesion sites. The real sample acquisition time is shown in seconds (time between frames = 1 s). Video 8 shows direct dual-color TIRFM visualization of microtubules targeting to adhesion sites. This movie accompanies Fig. 5 D and shows a CAR fibroblast double transfected with DsRed-zyxin (red) and GFP-tubulin (green) and simultaneously imaged by TIRFM using an emission splitter device (Optical Insights). The real sample acquisition time is shown in seconds (time between frames = 1 s). Online supplemental material available at <http://www.jcb.org/cgi/content/full/jcb.200301102/DC1>.

We thank Emmanuel Vignal for his invaluable graphic assistance with Fig. 5 E.

This work was supported by grants from the Austrian Science Foundation (P14007-BIO; J.V. Small), the Ludwig Institute for Cancer Research (D.K. Toomre), and the Max Planck Society and the Volkswagen-Stiftung (D.J. Manstein).

Submitted: 24 January 2003

Revised: 22 April 2003

Accepted: 22 April 2003

References

- Axelrod, D. 1989. Total internal reflection fluorescence microscopy. *Methods Cell Biol.* 30:245–270.
- Gavin, R.H. 1997. Microtubule-microfilament synergy in the cytoskeleton. *Int. Rev. Cytol.* 173:207–242.
- Geiger, B., and A. Bershadsky. 2001. Assembly and mechanosensory function of focal contacts. *Curr. Opin. Cell Biol.* 13:584–592.
- Goode, B.L., D.G. Drubin, and G. Barnes. 2000. Functional cooperation between the microtubule and actin cytoskeletons. *Curr. Opin. Cell Biol.* 12:63–71.
- Gundersen, G.G. 2002. Evolutionary conservation of microtubule-capture mechanisms. *Nat. Rev. Mol. Cell Biol.* 3:296–304.
- Kaverina, I., K. Rottner, and J.V. Small. 1998. Targeting, capture, and stabilization of microtubules at early focal adhesions. *J. Cell Biol.* 142:181–190.
- Kaverina, I., O. Krylyshkina, and J.V. Small. 1999. Microtubule targeting of substrate contacts promotes their relaxation and dissociation. *J. Cell Biol.* 146:1033–1044.
- Kaverina, I., O. Krylyshkina, and J.V. Small. 2002a. Regulation of substrate adhesion dynamics during cell motility. *Int. J. Biochem. Cell Biol.* 34:746–761.
- Kaverina, I., O. Krylyshkina, K. Beningo, K. Anderson, Y.-L. Wang, and J.V. Small. 2002b. Tensile stress stimulates microtubule outgrowth in living cells. *J. Cell Sci.* 115:2283–2291.
- Krendel, M., F.T. Zenke, and G.M. Bokoch. 2002. Nucleotide exchange factor GEF-H1 mediates cross-talk between microtubules and the actin cytoskeleton. *Nat. Cell Biol.* 4:294–301.
- Mimori-Kiyosue, Y., N. Shiina, and S. Tsukita. 2000. The dynamic behavior of the APC-binding protein EB1 on the distal ends of microtubules. *Curr. Biol.* 10:865–868.

- Perez, F., G.S. Diamantopoulos, R. Stalder, and T.E. Kreis. 1999. CLIP-170 highlights growing microtubule ends in vivo. *Cell* 96:517–527.
- Rickard, J.E., and T.E. Kreis. 1990. Identification of a novel nucleotide-sensitive microtubule-binding protein in HeLa cells. *J. Cell Biol.* 110:1623–1633.
- Rottner, K., M. Krause, M. Gimona, J.V. Small, and J. Wehland. 2001. Zyxin is not colocalized with vasodilator-stimulated phosphoprotein (VASP) at lamellipodial tips and exhibits different dynamics to vinculin, paxillin, and VASP in focal adhesions. *Mol. Biol. Cell.* 12:3103–3113.
- Schroer, T.A. 2001. Microtubules don and doff their caps: dynamic attachments at plus and minus ends. *Curr. Opin. Cell Biol.* 13:92–96.
- Schuyler, S.C., and D. Pellman. 2001. Microtubule “plus-end-tracking proteins”: the end is just the beginning. *Cell*. 105:421–424.
- Small, J.V., and I. Kaverina. 2003. Microtubules meet substrate adhesions to arrange cell polarity. *Curr. Opin. Cell Biol.* 15:40–47.
- Small, J.V., B. Geiger, I. Kaverina, and A. Bershadsky. 2002. Opinion: How do microtubules guide migrating cells? *Nat. Rev. Mol. Cell Biol.* 3:957–964.
- Steyer, J.A., and W. Almers. 2001. A real-time view of life within 100 nm of the plasma membrane. *Nat. Rev. Mol. Cell Biol.* 2:268–275.
- Toomre, D., and D.J. Manstein. 2001. Lighting up the cell surface with evanescent wave microscopy. *Trends Cell Biol.* 11:298–303.
- Toomre, D., J.A. Steyer, P. Keller, W. Almers, and K. Simons. 2000. Fusion of constitutive membrane traffic with the cell surface observed by evanescent wave microscopy. *J. Cell Biol.* 149:33–40.
- Truskey, G.A., J.S. Burmeister, E. Grapa, and W.M. Reichert. 1992. Total internal reflection fluorescence microscopy (TIRFM). II. Topographical mapping of relative cell/substratum separation distances. *J. Cell Sci.* 103:491–499.
- Vasiliev, J.M. 1985. Spreading of non-transformed and transformed cells. *Biochim. Biophys. Acta.* 780:21–65.
- Wittmann, T., and C.M. Waterman-Storer. 2001. Cell motility: can Rho GTPases and microtubules point the way? *J. Cell Sci.* 114:3795–3803.
- Yin, H., D. Pruyne, T.C. Huffaker, and A. Bretscher. 2000. Myosin V orientates the mitotic spindle in yeast. *Nature.* 406:1013–1015.